http://dx.doi.org/10.5012/bkcs.2013.34.5.1388

Synthesis and Characterization of New Macroporous SnO_2 Foams

Moon-Hyung Choi and Seung-Min Paek*

Department of Chemistry and Green-Nano Materials Research Center, Kyungpook National University, Taegu 702-701, Korea
**E-mail: smpaek@knu.ac.kr*
Received January 21, 2013, Accepted February 9, 2013

Macroporous SnO_2 foam was successfully synthesized *via* a simple soft-chemical route by hybridization between alkylamine and tin(IV) oxide. According to X-ray diffraction (XRD) analysis, the as-prepared SnO_2 foam had a highly ordered lamella structure along the crystallographic *c*-axis, which transformed to a rutile phase after thermal treatment at 300 °C. X-ray absorption spectroscopy (XAS) at the Sn *K*-edge revealed that SnO_2 particles in the hybrid material maintained their nanosized structure after hybridization with alkylamine. Scanning electron microscope (SEM) images clearly showed that the as-prepared SnO_2 foam had a macroporous structure. This synthetic route can be extended to the development of open frameworks with good electrochemical properties in battery applications.

Key Words : X-ray absorption spectroscopy, Layered material, Hybrid

Introduction

Recently, lithium ion batteries (LIBs) have attracted considerable attention owing to their high energy density and high electromotive force as power sources for electrical/hybrid vehicles and portable electronic devices.[1,2] In commercial LIBs, graphite is normally employed as a standard anode material because of its reversible charge/discharge reaction with a reasonable specific capacity of 372 mAh/g.[3,4] On the other hand, new anode materials with high energy densities and large specific capacities are needed to meet the increasing demand for batteries with enhanced electrochemical properties. In this regard, a transition metal oxide such as tin oxide (SnO_2) might be one of fascinating alternative anode materials in LIBs because of its very high theoretical Li^+ storage capacity of about 800 mAh/g.[5] Therefore, much research attempt has been made to obtain new SnO_2-based anode materials.[6-8]

Although SnO_2 has a very high theoretical specific capacity, its inherent drawback is that tin oxide shows a very large volume change of approximately 300% upon charge/discharge reactions.[9] Such drastic changes in volume result in cracking and crumbling of the electrodes, which leads to the electrical disconnection of tin oxide from the current collector as well as rapid capacity fading. To overcome these inherent drawbacks, nanostructured tin oxide materials with the enhanced cyclability have been widely explored, and a range of synthetic routes have been reported so far. For example, hollow tin oxide mesospheres were produced *via* a solvothermal synthesis,[10] and tin oxide nanotubes were fabricated from a soft-chemical process.[11] As a reliable alternative synthetic method, hybridization between organic molecules and inorganic metal oxides could be used to prepare a macroporous hybrid structure.[12] In this study, we demonstrated the synthesis of SnO_2 foam based on the electrostatic attraction between tin oxide precursors and long-chain alkylamines. The key strategy is to develop a new macroporous electrode material with large void spaces because macropores in a hybrid material can be used as buffered spaces during a volume change in charge/discharge reaction.

Experimental

Tin oxide foam was synthesized using the following procedure: tin(IV) chloride pentahydrate ($SnCl_4 \cdot 5H_2O$) was reacted with 1-hexadecylamine in acetone, where the molar ratio of tin(IV) chloride pentahydrate to 1-hexadecylamine was fixed to 2:3. The reaction mixture was stirred for 30 min to obtain a pasty mixture, which was followed by the addition of a 30 wt % aqueous solution of hydrogen peroxide. The evolution of oxygen gas caused by the decomposition of H_2O_2 led to the spontaneous formation of tin oxide foam. The reaction temperature was maintained at 70 °C. The rapid increase in the volume of products was observed, and the final volume of tin oxide foam after 20 min was determined to be approximately 500 mL. The product (tin oxide foam) was collected, and heat-treated at various temperatures from 100 to 300 °C. According to density measurements, the density of as-prepared sample was 0.461 g/cm^3 after drying whereas that of 300 °C-treated sample was 0.971 g/cm^3, which are much smaller than that of bulk SnO_2.

All the X-ray diffraction (XRD) patterns were obtained with a powder X-ray diffractometer (Bruker D2 phaser) using Ni-filtered Cu K_α radiation (λ = 1.5418 Å). High resolution transmission electron microscope (HRTEM) study was carried out with a Hitachi H-7600 at an accelerating voltage of 120 kV after the product embedded in a resin was ultramicrotomed into thin slices with a diamond knife. The morphology of the sample was examined using scanning electron microscope (SEM, Hitachi S-4300). X-ray absorption spectroscopy (XAS) experiments at the Sn K-edge were

carried out at the X-ray absorption fine structure (XAFS-II) facility installed at beamline 7D in Pohang Accelerator Laboratory (PAL), Korea. All the present spectra were calibrated by measuring the spectra of Sn metal foil simultaneously with those of the samples. Data analysis using UWXAFS 2.0 code was performed by the standard procedure as reported previously.[13-16]

Results and Discussion

Figures 1 and 2 demonstrate the crystal structure of tin oxide foam and heat-treated samples. The as-prepared hybrid sample clearly shows a series of well-defined (00*l*) reflections due to a preferred orientation of 1-hexadecylamine molecules, indicating a highly ordered lamella structure of this sample along the crystallographic *c*-axis. The alkyl chains of hexadecylamine in the hybrid could make the most stable layered conformation through the maximization of Van der Waals forces between alkyl chains. The (001) diffraction peak for the as-prepared sample was observed at 3.3°, which corresponds to the basal spacing of 2.5 nm. Considering this repeating unit and the length of 1-hexadecylamine (~2.0 nm),[17] the hexadecylamine might be arranged into monolayer with a tilt angle between tin oxide particles. Successive thermal treatments were performed to examine the thermal stability of this sample. This layered hybrid material maintains its lamellar structure up to 200 °C as shown in Figure 1(c). Heat-treatment at 250 °C resulted in the collapse of the ordered structure, which can be observed from the disappearance of (00*l*) reflections in the low angle region. The 250 °C-treated sample (Figure 2(a)) showed broad XRD peaks at 26.9, 34.1, and 51.9° due to the crystallization of tin oxide with a rutile phase. In the XRD pattern of a sample heat-treated at 300 °C (Figure 2(b)), the diffraction peak centered at 2θ = 26.9° can be also attributed to the rutile (110) reflection, supporting that amorphous SnO_2 nanopaticles are gradually transformed into rutile phase. From the the Scherrer formula analysis,[18] it is found that the average particle size of the sample heat-treated at 300 °C was determined to be about 20 nm, showing that SnO_2 nanopaticles in the hybrid materials maintain their small sizes even after thermal treatment. In addition, the cross-sectional HRTEM image of as-prepared hybrid sample was shown in the inset of Figure 2. This HRTEM image is composed of dark and bright fringes with regular repeating units. This result supports the typical layered structure of this product, as expected from XRD analysis.

Because the XRD patterns of the layered samples only provide the periodical *d*-spacing and long-ranged order of these samples, it is difficult to know the local structural variations of tin oxide in the samples during the thermal treatment. Therefore, we also examined the XAS spectra of the representative samples since the XAS analysis can provide valuable information on the local environment around

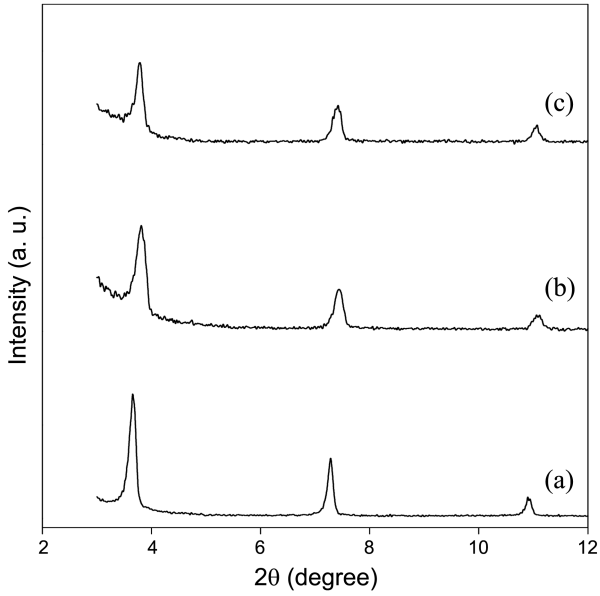

Figure 1. XRD patterns for (a) the as-prepared hybrid, (b) the hybrid heat-treated at 100 °C, and (c) the hybrid heat-treated at 200 °C.

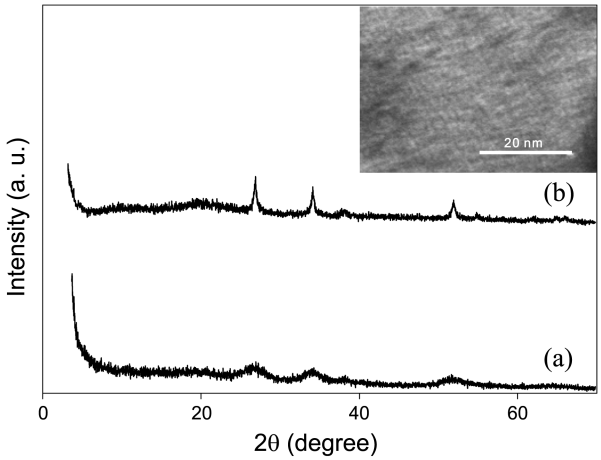

Figure 2. XRD patterns for (a) the hybrid heat-treated at 250 °C, (b) the hybrid heat-treated at 300 °C (inset: HRTEM image of the as-prepared hybrid)

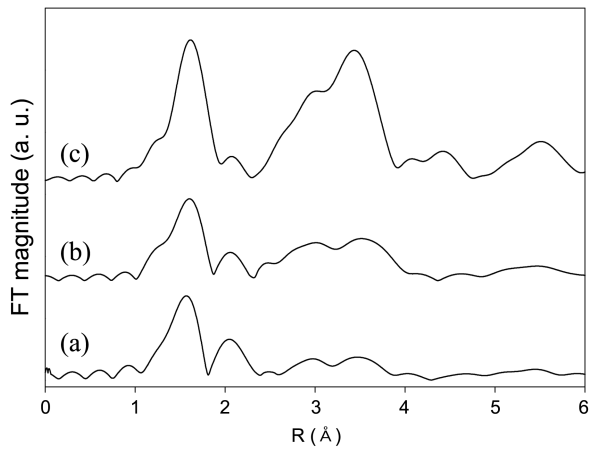

Figure 3. The Fourier transforms of the Sn K-edge EXAFS spectra for (a) the as-prepared hybrid, (b) the hybrid heat-treated at 300 °C, and (c) the bulk SnO_2 reference.

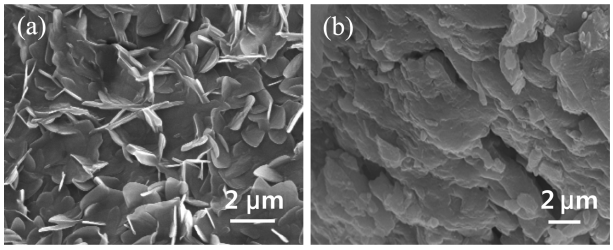

Figure 4. SEM images for (a) the as-prepared hybrid, (b) the hybrid heat-treated at 300 °C.

tin atoms in the hybrid. Figure 3 presents the Fourier transforms (FTs) of the Sn K-edge extended X-ray absorption fine structure (EXAFS) spectra of the samples, along with that of bulk SnO_2 as a reference. The peaks at 1.6, 2.9, and 3.4 Å in FTs (non-phase-shift-corrected) were assigned to the contribution of Sn–O, edge-shared Sn–Sn, and corner-shared Sn–Sn, respectively. The FT amplitude of the first shell of the as-prepared sample was much smaller than that of the bulk SnO_2 reference, highlighting the nanostructured nature of this sample. The SnO_6 octahedra in the as-prepared sample with a very small particle size must have less continuous surfaces and higher surface curvature, which results in smaller neighboring atoms and a smaller FT amplitude. Furthermore, it is noticeable that the FT peaks at 4-6 Å due to the multiple scattering paths were almost suppressed in the as-prepared sample, which originated from the smaller coordination numbers and nanocrystalline characteristics. On the other hand, the overall spectral features of the hybrid heat-treated at 300 °C resemble those of the bulk SnO_2 with a rutile crystal structure, which is in good agreement with the XRD analysis. On the other hand, as shown in Figure 3(b), the FT amplitudes of the second and third shell of this heat-treated sample were still much smaller than those of the bulk reference. Such spectral characteristics confirm that the SnO_2 in the present hybrid had maintained its nanosized features even after thermal treatment.

The SEM images of the samples are demonstrated in Figure 4. It is apparent that these hybrid materials showed a clear lamellar morphology, as expected from XRD and TEM observations. As shown in Figure 4(a), the as-prepared sample exhibited the stacks of loosely packed plates, where the lateral sizes of the plates are approximately several micrometers. The thickness of these plates can be determined to be about few tens of nanometers. Such morphological features lead to the macroporosity observed in this material. For this reason, this macroporous hybrid synthesized by a soft-chemical route is expected to be considerably more tolerant to volume changes during charge/discharge for battery applications, compared to the bulk SnO_2. After the thermal treatment of the sample at 300 °C, the agglomeration of plates was observed due to the collapse of macroporous structure. Studies examining the electrochemical properties of the samples are currently underway.

Conclusion

New tin oxide foam was obtained from hybridization between organic hexadecylamine molecules and inorganic SnO_2 nanoparticles. According to the XRD and TEM analysis, this hybrid sample shows a highly ordered lamella structure. XAS results reveal that tin oxide in hybrid samples maintained its nanosized nature even after a thermal treatment at 300 °C. From SEM images of samples, it was found that the as-prepared hybrid is composed of very thin plates. This soft-chemical synthetic route can be used for the synthesis of new nanostructured materials with open frameworks.

Acknowledgments. This research was supported by Kyungpook National University Research Fund (2010).

References

1. Whittingham, M. S. *Chem. Rev.* **2004**, *104*, 4271.
2. Armand, M.; Tarascon, J.-M. *Nature* **2008**, *451*, 652.
3. Wu, Y. P.; Rahm, E.; Holze, R. *J. Power Sources* **2003**, *114*, 228.
4. Buqa, H.; Goers, D.; Holzapfel, M.; Spahr, M. E.; Novak, P. *J. Electrochem. Soc.* **2005**, *152*, A474.
5. Courtney, I. A.; Dahn, J. R. *J. Electrochem. Soc.* **1997**, *144*, 2045.
6. Guo, H.; Mao, R.; Yang, X. J.; Wang, S. X.; Chen, J. *J. Power Sources* **2012**, *219*, 280.
7. Chen, J. S.; Archer, L. A.; Lou, X. W. *J. Mater. Chem.* **2011**, *21*, 9912.
8. Paek, S. M.; Yoo, E.; Honma, I. *Nano Lett.* **2009**, *9*, 72.
9. Brousse, T.; Retoux, R.; Herterich, U.; Schleich, D. M. *J. Electrochem. Soc.* **1998**, *145*, 1.
10. Deng, D.; Lee, J. Y. *Chem. Mater.* **2008**, *20*, 1841.
11. Zhao, N. H.; Wang, G. J.; Huang, Y.; Wang, B.; Yao, B. D.; Wu, Y. P. *Chem. Mater.* **2008**, *20*, 2612.
12. Chandrappa, G. T.; Steunou, N.; Livage, J. *Nature* **2002**, *416*, 702.
13. Paek, S. M.; Jung, H.; Park, M.; Lee, J. K.; Choy, J. H. *Chem. Mater.* **2005**, *17*, 3492.
14. Paek, S. M.; Jung, H.; Lee, Y. J.; Park, M.; Hwang, S. J.; Choy, J. H. *Chem. Mater.* **2006**, *18*, 1134.
15. Kang, J. H.; Paek, S. M.; Hwang, S. J.; Choy, J. H. *J. Mater. Chem.* **2010**, *20*, 2033.
16. Kang, J. H.; Paek, S. M.; Choy, J. H. *Bull. Kor. Chem. Soc.* **2010**, *31*, 3675.
17. Alba, M. D.; Castro, M. A.; Orta, M. M.; Pavón, E.; Pazos, M. C.; Rios, J. S. V. *Langmuir* **2011**, *27*, 9711.
18. Cullity, B. D. *Elements of X-Ray Diffraction*, 2nd ed.; Addison-Wesley: Reading, MA, 1977.